GAP JUNCTION STRUCTURES

III. THE EFFECT OF VARIATIONS IN THE ISOLATION PROCEDURE

LEE MAKOWSKI
Department of Biochemistry, College of Physicians and Surgeons of Columbia University, New York, New York 10032 U.S.A.

D. L. D. CASPAR
Rosenstiel Basic Medical Sciences Research Center, Brandeis University, Waltham, Massachusetts 02254 U.S.A.

D. A. GOODENOUGH
Department of Anatomy, Harvard Medical School, Boston, Massachusetts 02115 U.S.A.

W. C. PHILLIPS
Rosenstiel Basic Medical Sciences Research Center, Brandeis University, Waltham, Massachusetts 02254 U.S.A.

The structures of gap junctions isolated from mouse livers using two different protocols have been studied using x-ray diffraction. The second protocol differs from the first in using the detergent Brij 58 and requiring no exogenous proteases (2). The lattice constant of the two-dimensional hexogonal array of connexons varies between 74–84 Å in junctions isolated using the second protocol compared to 80–88 Å observed in junctions isolated using the earlier protocol. The Brij 58 appears to solubilize some of the junctional lipid causing closer packing of the connexons and an increase in the spatial ordering of connexons in the junctional lattice. Furthermore, the changes in the connexon structure within the gap region that were found to be correlated to lattice constant differences (1, 3) are not observed in junctions isolated using the Brij 58 protocol.

Sharp x-ray reflections from specimens with lattice constants of ~ 80 Å or less are usually observed out to the (4,0) reflection and the sampling of the equatorial transform is apparent out to 7 Å spacing in some diffraction patterns. Strong diffraction is observed near the meridian at ~ 4.7 Å spacing and at ~ 10 Å spacing on the equator. This combination of diffraction is characteristic of the cross-β protein conformation, suggesting that a significant portion of the junction protein may be in a β-sheet conformation.

Structural changes have been found that correspond to variations in the Brij 58 protocol. The addition of deoxycholate during isolation usually reduces the observed lattice constant by 2–4 Å. Addition of trypsin or chymotrypsin removes protein from the cytoplasmic surfaces but does not alter the 4.7 Å diffraction from the interior of the connexon. Addition of EGTA to the initial homogenization increases the yield of the isolation procedure by a factor of ~ 10. Junctions isolated with EGTA form much more extensive, better-ordered lamellar stacks than those

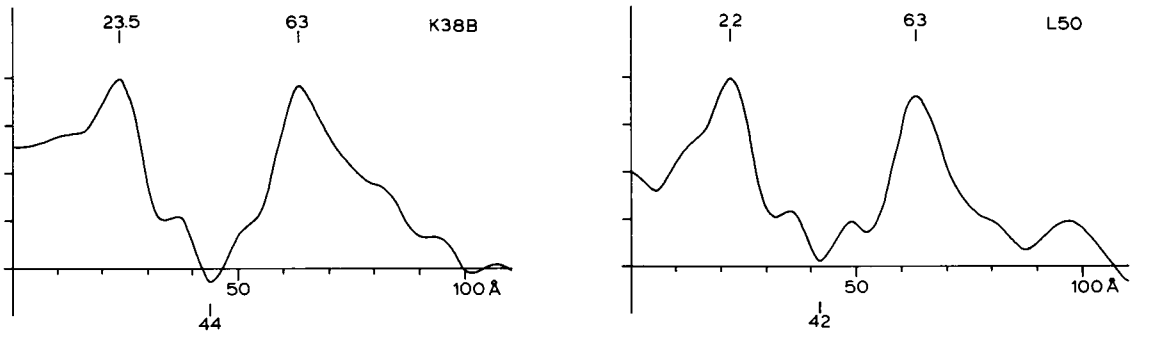

FIGURE 1 Electron density profiles of isolated gap junctions determined by analysis of x-ray diffraction data to 10 Å resolution. (*a*) Specimen K38B was isolated using the Brij 58 protocol without EGTA in the initial homogenization. (*b*) Specimen L50 was isolated in the same manner as K38B with eGTA in the initial homogenization. Only one of the two membranes making up the gap junction is shown in these drawings. Dimensions marked are distances from the center of the gap which is at the left edge of the electron density profiles. Differences in the structure of the junctions in these two specimens are apparent in the distribution of electron density near the cytoplasmic surface of the junctions (80–110 Å from the gap) and in the distance between the two electron dense polar head groups.

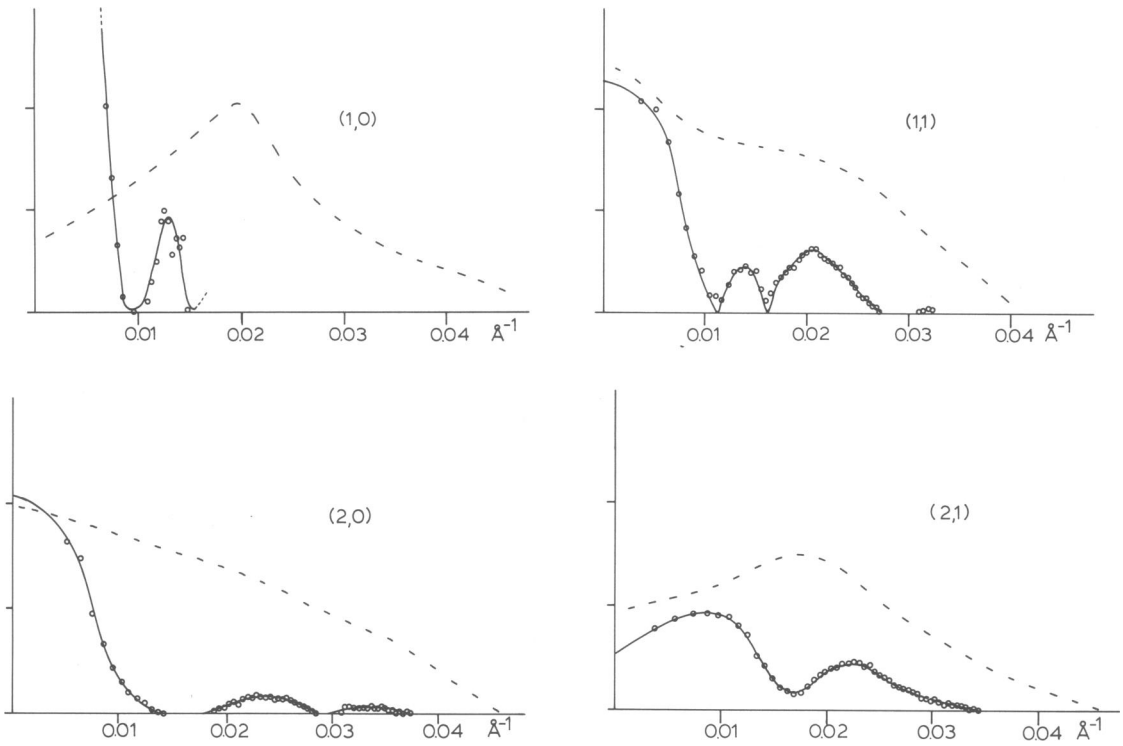

FIGURE 2 Comparson of lattice line data from x-ray diffraction and electron microscopy of isolated mouse liver gap junctions. (-o-) are uncorrected intensities calculated from x-ray diffraction patterns from gap junctions using angular deconvolution. (--) (not to scale) are electron microscope data (5).

isolated without EGTA. They also have a different distribution of mass on the cytoplasmic surface. The junctions isolated with EGTA stack in the x-ray specimens with a center-to-center spacing of ~ 170 Å even though electron density extends out from the center of the gap 105–110 Å. This means that the total width of the junction is > 200Å from one cytoplasmic surface to the next and that the junctions are capable of interleaving with one another in the x-ray specimens.

In Fig. 1, electron density profiles of two gap junction specimens are presented, one isolated with EGTA (L50) and one without (K38B). There are several structural differences between the two profiles. In L50, a large peak of electron density at 95–105 Å from the center of the gap, missing in K38B, indicates that the connexons extend further into the cytoplasm in junctions isolated with EGTA than without. Differences in the lipid bilayers, in particular the separation between polar head groups, suggest that the two specimens may have different lipid compositions. These structural differences may be due to structural changes induced by the EGTA or by the selection of two different subpopulations of junctions due to the differential action of EGTA on junctions with slightly different structures.

Several specimens have been produced with sufficiently good orientation to allow measurement of diffraction data along lattice lines to ~ 30 Å resolution using angular deconvolution (4). The x-ray intensities along lattice lines

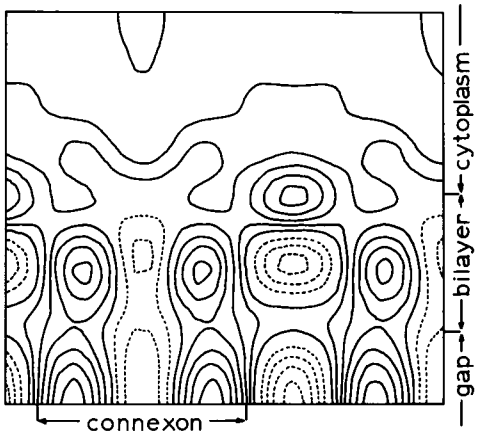

FIGURE 3 Section through a three-dimensional electron density map of isolated gap junctions. The cytoplasm is towards the top, the center of the extracellular gap is along the bottom. (--) represent troughs in the electron density; (—) represent peaks. Two images of the transmembrane channel are present, one along the right-hand edge and one in the center of the connexon in the left-hand half of the figure. This map was calculated using the intensities in Fig. 2 (after correction) and the phase choice that produced the electron density map most consistent with the results of electron microscopy and the known bilayer structure of the membrane lipids. Because of the P622 symmetry of the junction lattice, the amplitudes are real on all lattice lines (h, k) for which $h = k$, or $h = 0$, or $k = 0$. Of the lattice lines along which data were measured, only the (2, 1) has complex amplitudes. The phases of the lattice lines at the equator were determined previously by correlation to the electron microscopy (3). These considerations limited the number of phase choices which had to be considered in the construction of this map.

are very different from the data collected using electron microscopy of negatively stained gap junctions (5). In Fig. 2, the x-ray intensities are plotted along with the approximate electron microscope measurements. The x-ray data have substantially higher frequency detail along lattice lines than the electron microscope data because the principal contrast seen in the electron microscope is the 30-Å thick layer of stain in the extracellular gap, whereas the principal contrast for x-rays is the 150-Å thick protein unit. In Fig. 3, a single section of a three-dimensional electron density map of a gap junction specimen is presented. This section is perpendicular to the membrane plane and cuts through the centers of two connexons. The cytoplasm is at the top and the center of the gap is at the bottom. The channel through the center of the connexon can be seen extending most of the way from the center of the gap to the cytoplasmic surface. The channel may not extend entirely through the junction to the cytoplasm. Analysis of diffraction patterns from isolated gap junctions in 50% sucrose shows that the sucrose fills the extracellular gap but fails to enter the channel. It is possible that the channel is closed at both cytoplasmic surfaces, excluding sucrose. This suggests that the isolated junctions are in a high resistance state.

Received for publication 18 May 1981.

REFERENCES

1. Caspar, D. L. D., D. A. Goodenough, L. Makowski, and W. C. Phillips. 1977. Gap junction structures. I. Correlated electron microscopy and x-ray diffraction. *J. Cell Biol.* 74:605.
2. Fallon, R. F., and D. A. Goodenough. 1981. Bulk isolation of mouse hepatocyte gap junctions. *J. Cell Biol.* In press.
3. Makowski, L., D. L. D. Caspar, W. C. Phillips, and D. A. Goodenough. 1977. Gap junction structures. II. Analysis of the x-ray diffraction data. *J. Cell Biol.* 74:629.
4. Makowski, L. 1978. Processing of x-ray diffraction data from partially oriented specimens. *J. Appl. Cryst.* 11:273.
5. Unwin, P. N. T., and G. Zampighi. 1980. Structure of the junctions between communicating cells. *Nature (Lond.).* 283:545.

ON THE STRUCTURAL ROLE OF THE ε-(γ-GLUTAMYL)LYSINE CROSS-LINK IN THE CELL MEMBRANE

R. B. HAUGLAND, T-I. LIN, R. M. DOWBEN, AND P. J. BIRCKBICHLER
Department of Pathology, Baylor University Medical Center, Dallas, Texas 75246 and Biomedical Division, S. Roberts Nobel Foundation, Ardmore, Oklahoma 73401 U.S.A.

We were first to show (1) that membrane proteins obtained from tissue-cultured cells contain significant amounts of isopeptide bonds between the ε-amino groups of lysine and the γ-carboxyl groups of glutamate. These bonds are formed as cross-links between membrane proteins by a Ca^{2+}-activated transglutaminase similar to blood clotting factor XIII present in plasma. Rigid structures such as wool and hair are quite rich in Glu-Lys isopeptide bonds (2). Nonproliferating cell membranes contain more isopeptide bonds than those of actively dividing cells, suggesting that one function of Glu-Lys is to stabilize the cell membrane and contribute to the termination of cell division (3).

Staining nonproliferating fibroblasts with transglutaminase antibodies (4) showed that transglutaminase is a membrane-associated enzyme. Thus, it is possible that Glu-Lys cross-links are involved in maintaining the "architecture" of the cell membrane in relation to cell shape and function.

MATERIALS AND METHODS

To investigate these possibilities, we grew L cells (NTC 929) or maintained surviving cultures of mouse ascites cells (Lettre) in the presence of one of two alternative substrates for the transglutaminase that prevent Glu-Lys cross-linking, cystamine or dansylcadaverine. Experiments were also performed in the presence of the Ca^{2+} ionophore A_{23187} which enhances cross-linking by increasing the concentration of Ca^{2+} intracellularly.

The structure of the cell membrane was studied four with fluorescent probes: 12-(9-anthroyloxy)stearic acid (12-AS); 2-(9-anthroyloxy)stearic acid (2-AS); 1,6-diphenyl-1,3,5-hexatriene (DPH); and 1-(4-trimethylammoniumphenyl)-6-phenyl-1,3,5-hexatriene (TMA-DPH). Fluorescence polarization and lifetime measurements were used to compare quantitatively the localized environment of the cell membrane under various conditions (5). Cell membrane fragments were prepared by nitrogen cavitation (6). Na^+,K^+-activated ATPase activity was determined in the presence and absence of 0.1 mM ouabain by a NADH oxidation-linked system (7). Glu-Lys was measured as described by Birckbichler et al. (3). Cholesterol was assayed using a kit supplied by Abbott Diagnostics (S. Pasadena, CA). Fluorescence polarization was measured with a photon counting system, and fluorescence lifetimes by a nanosecond pulse fluorimeter using single photon counting, both instruments constructed in our laboratory. The probes were used at a molar ratio of ~1:200 total lipid.

RESULTS

We observed a time-related decrease in the Glu-Lys content of membranes of cells grown in the presence of 0.1 mM dansylcadaverine or 1.0 mM cystamine (Fig. 1). A slight increase of Glu-Lys was found in cells treated with 0.5×10^{-6} M A_{23187}, a smaller increase than other investigators found in red blood cells (5), but we could not use